

Ch. RamReddy*, O. Surender, and Ch. Venkata Rao

Effects of Soret, Hall and Ion-slip on mixed convection in an electrically conducting Casson fluid in a vertical channel

DOI 10.1515/nleng-2016-0016

Received April 5, 2016; accepted May 12, 2016.

Abstract: The significance of Soret, Hall and Ion-slip effects on mixed convection flow of an electrically conducting Casson fluid in a vertical channel in the presence of viscous dissipation is analyzed. The system of flow governing equations are converted into the system of non-dimensional equations using appropriate non-dimensional transformations and hence solved analytically by homotopy analysis method. A quantitative comparison is made between homotopy analysis method and Adomian decomposition method and the results are found to be in good agreement. The dimensionless velocity, temperature and species concentration profiles are illustrated graphically and quantitatively with special focus on the Casson fluid, Soret, viscous dissipation, Hall and Ion-slip parameters.

Keywords: Mixed convection; Casson fluid; Soret effect; Vertical channel; Viscous dissipation; Homotopy analysis method

1 Introduction

In view of the broad range of applications such as lubrication system, polymer processing, chemical processing equipment, hydrodynamical machines, ventilation of buildings, electronic equipment, etc., the investigation of combined free convection and forced convection heat transfer and fluid momentum between two parallel plates has been regarded as one of the most important research topic. Tao [1] presented combined free convection and

forced convection of a fully developed flow in vertical channel with or without heat generation. Barletta [2] discussed the mixed convection flow in a parallel plates vertical channel with viscous dissipation effect. Several studies have been undertaken in the field of fluid flow and heat transfer between parallel plates. The flow and heat transfer of Newtonian and non-Newtonian fluids between two parallel plates are investigated by many researchers under various physical conditions [3–9].

With the emergent importance of non-Newtonian fluids in recent industries and technology, mathematical modeling of non-Newtonian fluid flows and their understanding are of both fundamental and practical significance. The most important non-Newtonian fluid, possessing a yield value below which no flow occurs and a zero viscosity at an infinite rate of shear, is the *Casson Fluid*, which has significant applications in polymer processing industries and biomechanics. The examples of Casson fluid are of the type are as follows: jelly, tomato sauce, honey, soup, concentrated fruit juices, etc. The constitutive equation of Casson fluid [10] represents a nonlinear relationship between stress and rate of strain. These fluids have been found to be accurately applicable to silicon suspensions, suspensions of bentonite in water and lithographic varnishes used for printing inks. The flow or/and heat transfer of a Casson fluid about different geometries have been reported by several researchers [11–17]. Further, at low shear rates when blood flows through small vessels, the blood flow is described by the Casson fluid model (McDonald [18]; Shaw *et al.* [19]). Mukhopadhyay [20] found that temperature increases with an increase in nonlinear stretching parameter and the momentum boundary layer thickness decreases with an increase in Casson parameter. The cross-diffusion effects on the stagnation-point flow of a non-Newtonian Casson fluid over a stretching sheet is investigated by Kameswaran *et al.* [21].

In recent times, due to increasing industrial applications, the flows involving thermal diffusion in non-Newtonian fluids grab significant attention of modern day researchers. In an initial homogeneous mixture, the growth of species differentiation subjected to a gradient of temperature is called Soret (or thermal-diffusion) effect.

*Corresponding Author: Ch. RamReddy: Department of Mathematics, National Institute of Technology Warangal-506004, India, E-mail: chittetiram@gmail.com; chramreddy@nitw.ac.in

O. Surender: Department of Mathematics, National Institute of Technology Mizoram-796012, India

Ch. Venkata Rao: Department of Mathematics, National Institute of Technology Warangal-506004, India

For example, Soret effect can be significant when species are introduced at a surface in fluid domain, with a density lower than the surrounding fluid. Eckert and Drake [22] have pointed out that in a convective fluid one cannot neglect the thermal-diffusion effect when the flow of mass is caused by a temperature difference, owing to its practical application such as hydrology, petrology, geosciences, etc. Dursunkaya and Worek [23] studied transient and steady natural convection from a vertical surface with diffusion-thermo and thermal-diffusion effects. Srinivasacharya and co-authors [24–26] (also see the citations therein) reported effect of Soret on convective boundary layer flow of various fluids by considering different surface geometries like vertical channel, vertical wavy surface and vertical plate.

Several researchers combined the MHD flow problems with Hall effect due to the reason that, when the strength of the magnetic field is strong, one cannot neglect the Hall current effect. The current component which flows in the direction mutually perpendicular to both the electric and magnetic induction fields is termed as the Hall current. Tani [27] considered the Hall effects on the steady motion of electrically conducting viscous fluid in channels. Influence of Hall and ion-slip in magneto hydrodynamic Couette flow with heat transfer has been discussed by Soundalgekar *et al.* [28]. The significant analysis regarding the Ion-slip and Hall effects in non-Newtonian fluids, one can refer the works of Srinivasacharya and Mekonnen [29–31]. Influence of Hall and Ion-slip effects on fully developed mixed convection flow of couple stress fluid between parallel disks has been presented by Srinivasacharya and Kaladhar [32]. By considering a vertical porous channel, Garg *et al.* [33] examined the Hall effect in an electrically conducting viscoelastic fluid through a porous medium.

The aim of the present article is to investigate the combined effect of Soret and viscous dissipation on steady mixed convective flow of an electrically conducting Casson fluid in a vertical channel in the presence of Hall and Ion-slip parameters. This mathematical model may be helpful for possible technological applications in liquid-based systems involving materials. The Homotopy Analysis Method (HAM) is employed to solve the governing nonlinear equations. To assess the accuracy of our method, the solution is compared with the analytical solution obtained by Adomian decomposition method. The behavior of flow characteristics with pertinent flow parameters is discussed.

2 Formulation of the problem

Consider the steady, laminar and incompressible mixed convection flow of an electrically conducting Casson fluid between two vertical plates of distant $2d$ apart. Choose the coordinate system such that x -axis be taken along vertically upward direction through the central line of the channel, y -axis is perpendicular to the plates and the two plates infinitely extended in the direction of x and z as shown in the flow configuration Fig. 1. The plate at distance $-d$ is maintained at a constant temperature and concentration T_1 and C_1 , while the plate at d at a constant temperature and concentration T_2 and C_2 . In comparison with the applied magnetic field, the induced magnetic field can be neglected on the assume that the magnetic Reynolds number is very small and the flow is steady and imposition of uniform pressure gradient in the direction of x . The effect of Ion-slip and Hall current gives rise to force in the z -direction, which induces a cross flow in that direction and hence the flow becomes three dimensional.

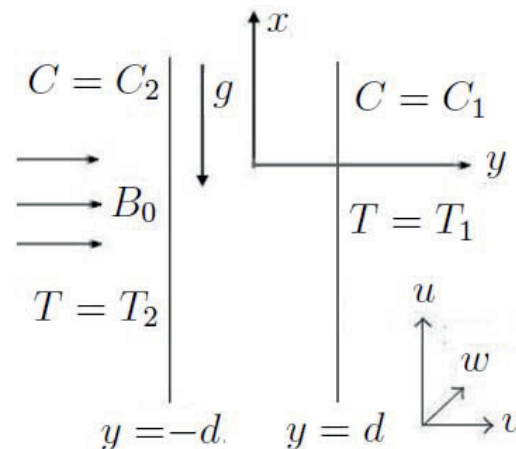


Fig. 1: Physical model and coordinate system.

By employing the Boussinesq and the standard boundary layer approximations, and making use of the above assumptions, the governing equations of mixed convection flow of an electrically conducting Casson fluid in the presence of viscous dissipation and Soret effects are given by

$$\frac{\partial v}{\partial y} = 0 \Rightarrow v = v_0 \quad (1)$$

$$\begin{aligned} \rho v \frac{\partial u}{\partial y} = -\frac{\partial P}{\partial x} + \mu \left(1 + \frac{1}{\beta}\right) \frac{\partial^2 u}{\partial y^2} \\ + g\rho [\beta_T(T - T_1) + \beta_C(C - C_1)] - \frac{\sigma B_0^2}{\alpha_e^2 + \beta_h^2} (\alpha_e u + \beta_h w) \end{aligned} \quad (2)$$

$$\rho v \frac{\partial u}{\partial y} = \mu \left(1 + \frac{1}{\beta}\right) \frac{\partial^2 w}{\partial y^2} + \frac{\sigma B_0^2}{\alpha_e^2 + \beta_h^2} (\beta_h u - \alpha_e w) \quad (3)$$

$$v \frac{\partial T}{\partial y} = \alpha \frac{\partial^2 T}{\partial y^2} + \frac{2\mu}{\rho C_p} \left[\left(\frac{\partial u}{\partial y}\right)^2 + \left(\frac{\partial w}{\partial y}\right)^2 \right] \quad (4)$$

$$v \frac{\partial C}{\partial y} = D \frac{\partial^2 C}{\partial y^2} + D_T \frac{\partial^2 T}{\partial y^2} \quad (5)$$

where u , v and w are velocity components along the x , y and z directions respectively, C_p is the specific heat capacity, μ is the coefficient of viscosity, ρ is the density, g is the acceleration due to gravity, σ is the electrical conductivity, B_0 is the magnetic field applied normal to the surface, K_T is the thermal diffusion ratio, β_h is Hall parameter, β_i is ion-slip parameter, $\alpha_e = 1 + \beta_h \beta_i$ is a constant, and β_T and β_C are the coefficients of thermal and solutal expansion, k is the coefficient of thermal conductivity, α is the thermal diffusivity, D is the mass diffusivity and T_m is the mean fluid temperature. The fluid velocity vector $\vec{q} = (u; v)$ is assumed to be parallel to the x -axis, so that only the x component u of the velocity vector does not vanish but the transpiration cross-flow velocity v_0 remains constant, where $v_0 < 0$ and $v_0 > 0$ are velocities of suction and injection, respectively. Finally β is the Casson fluid parameter and as $\beta \rightarrow \infty$ i.e. $\frac{1}{\beta} \rightarrow 0$, the governing equations of the Casson fluid model ($\beta \rightarrow \infty$) given by Eqs. (1)-(5) become the governing equations of the Newtonian fluid model ($\beta \rightarrow \infty$).

The boundary conditions are:

$$u = 0, \quad v = v_0, \quad w = 0, \quad T = T_1, \quad C = C_1 \quad \text{on } y = -d, \quad (6a)$$

$$u = 0, \quad v = v_0, \quad w = 0, \quad T = T_2, \quad C = C_2 \quad \text{on } y = d. \quad (6b)$$

Introducing the following transformations

$$\begin{aligned} \eta = \frac{y}{d}, \quad U = \frac{u}{u_0}, \quad W = \frac{w}{u_0}, \quad \theta = \frac{T - T_1}{T_2 - T_1}, \\ \phi = \frac{C - C_1}{C_2 - C_1}, \quad P = \frac{d^2 p}{\mu u_0} \end{aligned} \quad (7)$$

in Eqs. (1) - (5), we get the following system of nonlinear differential equations

$$\left(1 + \frac{1}{\beta}\right) U'' - RU' + \lambda(\theta + B\phi) - \frac{Ha^2}{\alpha_e^2 + \beta_h^2} (\alpha_e U + \beta_h W) - A = 0 \quad (8)$$

$$\left(1 + \frac{1}{\beta}\right) W'' - RW' + \frac{Ha^2}{\alpha_e^2 + \beta_h^2} (\beta_h U - \alpha_e W) = 0 \quad (9)$$

$$\theta'' - RPr\theta' + 2Br[(U')^2 + (W')^2] = 0 \quad (10)$$

$$\phi'' - RSc\phi' + Sr\theta'' = 0 \quad (11)$$

where the prime indicate differentiation with respect to η . In usual notations, $B = \frac{\beta_C(C_2 - C_1)}{\beta_T(T_2 - T_1)}$ is the regular buoyancy ratio, $Pr = \frac{\nu}{\alpha}$ is the Prandtl number and $Sc = \frac{\nu}{D}$ is the Schmidt number. Further, $R = \frac{v_0 d}{\nu}$ is the suction/injection parameter, $\lambda = \frac{Gr}{Re}$ is the mixed convection parameter, $Gr = \frac{g\beta_T(T_2 - T_1)d^3}{\nu^2}$ is the Grashof number, $Re = \frac{u_0 d}{\nu}$ is the Reynold's number, $Ha^2 = \frac{B_0^2 d^2 \sigma}{\mu}$ is the Hartman number and $A = \frac{d^2}{\mu u_0} \frac{\partial p}{\partial x}$ is a constant pressure gradient. Finally, $Br = \frac{\mu U_0^2}{k(T_2 - T_1)}$ is the Brinkman number and $Sr = \frac{D_{CT}(T_2 - T_1)}{\nu(C_2 - C_1)}$ is the Soret number.

Boundary conditions (6) in terms of U , W , θ and ϕ become

$$\begin{aligned} U = 0, \quad W = 0, \quad \theta = 0, \quad \phi = 0 \quad \text{at } \eta = -1 \\ U = 0, \quad W = 0, \quad \theta = 1, \quad \phi = 1 \quad \text{at } \eta = 1 \end{aligned} \quad (12)$$

The results of practical interest are the non-dimensional skin friction $C_f Re = 2 \left(1 + \frac{1}{\beta}\right) U'(\pm 1)$, the heat transfer rate $Nu = -\theta'(\pm 1)$, the mass transfer rate $Sh = -\phi'(\pm 1)$.

3 Adomian Decomposition Method(ADM) for the solution of the problem

The analytical solution of Eqs. (8) – (11) is given by the following (For more details of ADM, see Hakeri Askia *et al.* [34])

$$\begin{aligned} U(\eta) = a_1 + a_2 \eta + \left(1 + \frac{1}{\beta}\right) \times \\ \left[Ra_2 - \lambda(a_5 + Ba_7) + \frac{Ha_a^2}{\alpha_e^2 + \beta_h^2} (\alpha_e a_1 + \beta_h a_3) + A \right] \frac{\eta^2}{2} + \\ \left(1 + \frac{1}{\beta}\right) \left[-\lambda(a_6 + Ba_8) + \frac{Ha_a^2}{\alpha_e^2 + \beta_h^2} (\alpha_e a_2 + \beta_h a_4) \right] \frac{\eta^3}{6} + \dots \end{aligned} \quad (13)$$

$$W(\eta) = a_3 + a_4\eta + \left(1 + \frac{1}{\beta}\right) \times \left[Ra_4 - \frac{H_a^2}{\alpha_e^2 + \beta_h^2} (\beta_h a_1 - \alpha_e a_3) \right] \frac{\eta^2}{2} + \left(1 + \frac{1}{\beta}\right) \left[-\frac{H_a^2}{\alpha_e^2 + \beta_h^2} (\beta_h a_2 - \alpha_e a_4) \right] \frac{\eta^3}{6} + \dots \quad (14)$$

$$\theta(\eta) = a_5 + a_6\eta + \left[R Pr a_6 - 2Br(a_2^2 + a_4^2) \right] \frac{\eta^2}{2} + \dots \quad (15)$$

$$\phi(\eta) = a_7 + a_8\eta + \left[R Sc a_8 - Sr \left(R Pr a_6 - 2Br(a_2^2 + a_4^2) \right) \right] \frac{\eta^2}{2} + (R^2 Sc^2 a_8) \frac{\eta^3}{6} + \dots \quad (16)$$

For the complete solution of equations above, $a_1, a_2, a_3, a_4, a_5, a_6, a_7$ and a_8 should be determined with the help of boundary conditions (12).

4 The Homotopy Analysis Method (HAM) for the solution of the problem

In order to start any iterative solution, we have to choose the initial profiles of $U(\eta)$, $W(\eta)$, $\theta(\eta)$ and $\phi(\eta)$, and hence the initial profiles are taken as follows (For more details on homotopy analysis method and its efficient features, the readers can refer the works of Liao [35]–[37]):

$$U_0(\eta) = 0, W_0(\eta) = 0, \theta_0(\eta) = \frac{(\eta + 1)}{2} \text{ and } \phi_0(\eta) = \frac{(\eta + 1)}{2} \quad (17)$$

and choose the auxiliary linear operators:

$$L_i = \frac{\partial^2}{\partial \eta^2} \quad \text{for } i = 1, 2, 3, 4 \quad (18)$$

such that

$$L_1(c_1 + c_2\eta) = 0, L_2(c_3 + c_4\eta) = 0, L_3(c_5 + c_6\eta) = 0 \text{ and } L_4(c_7 + c_8\eta) = 0 \quad (19)$$

where $c_i (i = 1, 2, \dots, 8)$ are constants.

Since the non-zero convergence control parameters h_i , $i = 1, 2, 3, 4$ are introduced in zeroth-order deformation of the problem, the convergence and the rate of approximation for the HAM solution strongly depend on the values of auxiliary parameter h . Hence the non-linear operators N_i , $i = 1, 2, 3, 4$, the optimal values of h_i , $i = 1, 2, 3, 4$ at different order of approximations (see article by Liao [35] and [37]) and the average residual errors of $U(\eta)$, $W(\eta)$, $\theta(\eta)$ and $\phi(\eta)$ are examined clearly as

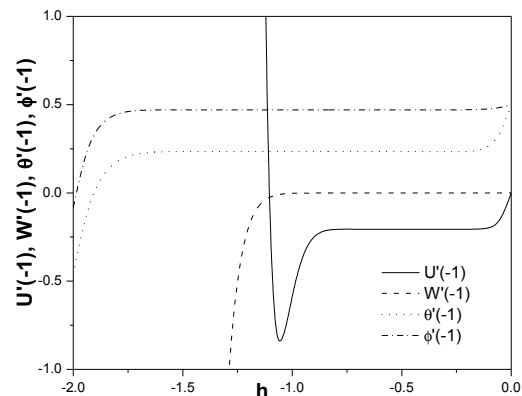


Fig. 2: The h -curves of $U'(\eta)$, $W'(\eta)$, $\theta'(\eta)$ and $\phi'(\eta)$ when $\beta = 1.0$, $Ha = 2.0$, $B = 1.0$, $R = 1.0$, $A = 1.0$, $Pr = 0.71$, $B_i = 2.0$, $Sc = 0.22$, $B_h = 2.0$, $Sr = 0.3$, $Br = 0.5$

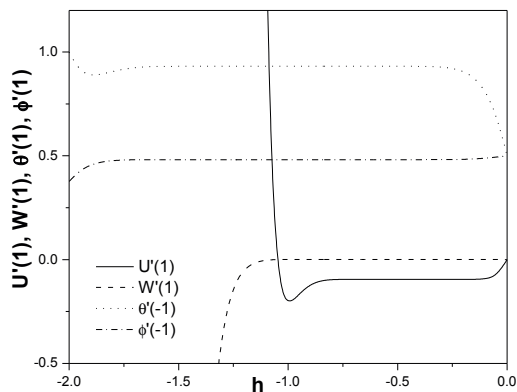
discussed in the works by Srinivasacharya and Kaladhar ([24]–[32]) and also citation therein.

To ensure the convergence and the admissible values of h_i , $i = 1, 2, 3, 4$, the h -curves are plotted for 18th-order of approximation in Figs. 2–3 by taking the values of the parameters $\beta = 1.0$, $Ha = 2.0$, $B = 1.0$, $R = 1.0$, $A = 1.0$, $Pr = 0.71$, $B_i = 2.0$, $Sc = 0.22$, $B_h = 2.0$, $Sr = 0.3$, $Br = 0.5$. It is evident from Figs. 2–3 that the h -curves have parallel line segments that corresponds to regions $-0.8 < h_1 < -0.15$, $-0.9 < h_2 < -0.1$, $-1.5 < h_3 < -0.4$ and $-1.5 < h_4 < -0.4$. To choose optimal value of auxiliary parameter from these wide ranges, the average residual errors are studied at different order of approximations (m), minimum of average residual errors are shown in Tables 2–5. From Table 2, we see that the average residual error for U is minimum at $h_1 = -0.37$. Table 3 shows that the minimum of average residual error for W attains at $h_2 = -0.59$. Table 4 depicts that at $h_3 = -1.06$, E_θ attains minimum. The average value of E_ϕ is minimum for $h_4 = -0.83$ as illustrated in Table 5. Therefore, the optimum values of convergence control parameters are taken as $h_1 = -0.37$, $h_2 = -0.59$, $h_3 = -1.06$ and $h_4 = -0.83$.

In order to assess the accuracy of our results, the accuracy between the solutions of the problem obtained by both Homotopy Analysis Method (HAM) for 18th order and Adomian Decomposition Method (ADM) for 8th order is presented in Tab. 1 and the results are found to be in very good agreement.

Table 1: Comparison of Cf_1 , Nu_1 , and Sh_1 between ADM and HAM when $B = 1.0$, $R = 1.0$, $A = 1.0$, $Pr = 0.71$, $B_i = 2.0$, $Sc = 0.22$, $B_h = 2.0$, $Sr = 0.3$, $Br = 0.5$.

λ	Ha	β	ADM for 8 th order			HAM for 18 th order		
			Cf_1	Nu_1	Sh_1	Cf_1	Nu_1	Sh_1
-1.0	1.0	1.0	-2.48745	-0.234362	-0.470365	-2.48737	-0.234387	-0.470373
0.0	1.0	1.0	-1.62982	-0.245020	-0.467809	-1.62971	-0.245035	-0.467813
1.0	1.0	1.0	-0.82429	-0.326308	-0.445933	-0.82419	-0.326325	-0.445938

**Fig. 3:** The h -curves of $U'(\eta)$, $W'(\eta)$, $\theta'(\eta)$ and $\phi'(\eta)$ when $\beta = 1.0$, $Ha = 2.0$, $B = 1.0$, $R = 1.0$, $A = 1.0$, $Pr = 0.71$, $B_i = 2.0$, $Sc = 0.22$, $B_h = 2.0$, $Sr = 0.3$, $Br = 0.5$ **Table 2:** Optimal value of h_1 at different order of approximations

Order	Optimal of h_1	Minimum of E_m
14	-0.37	5.51×10^{-16}
16	-0.39	5.89×10^{-18}
18	-0.37	2.41×10^{-19}

Table 3: Optimal value of h_2 at different order of approximations

Order	Optimal of h_2	Minimum of E_m
14	-0.6	4.81×10^{-19}
16	-0.59	9.31×10^{-22}
18	-0.6	1.24×10^{-23}

Table 4: Optimal value of h_3 at different order of approximations

Order	Optimal of h_3	Minimum of E_m
14	-1.06	7.46×10^{-16}
16	-1.05	3.20×10^{-17}
18	-1.06	2.69×10^{-19}

Table 5: Optimal value of h_4 at different order of approximations

Order	Optimal of h_4	Minimum of E_m
14	-0.83	4.19×10^{-16}
16	-0.89	4.24×10^{-18}
18	-0.83	6.35×10^{-20}

5 Results and discussion

The results of non-dimensional skin friction, Nusselt and Sherwood numbers at both the walls have been computed and illustrated graphically using the homotopy analysis method. In order to analyze the combined effects of Casson parameter (β), Magnetic parameter (Ha), Brinkman number (Br), Soret number (Sr), Hall and Ion-slip Parameters (β_i and β_h), computations are carried out in the cases of $B = 1.0$, $R = 1.0$, $A = 1.0$, $Pr = 0.71$, $Sc = 0.22$. These values are fixed through out the paper unless otherwise mentioned.

The variation of non-dimensional skin friction coefficient, heat and mass transfer rates against mixed convection parameter for different values of Hartman number Ha and Casson parameter β are depicted in Figs. 4(a)–4(c). Figure 4(a) reveals that, in the presence of both opposing and aiding flow situations, the skin friction coefficient enhances at left wall of the channel (i.e., surface at $y = -d$) and diminishes at right wall (i.e., surface at $y = d$) with increase in magnetic parameter Ha . Moreover, with rise in Casson parameter β , the skin friction coefficient show the same trend at both left and right walls of the channel. It is found that Newtonian fluid ($\beta \rightarrow \infty$) has less friction with wall compared to that of Casson fluid ($\beta \rightarrow \infty$) which is due to viscosity effects. In Fig. 4(b) for opposing and aiding flow cases, as the Casson parameter β increases, the heat transfer rate decreases at left wall and the opposite is true at right wall. With increase in magnetic parameter Ha , the heat transfer rate increases at left wall and decreases at right wall of the channel. Figure 4(c) illustrates that at right wall of the channel, the mass transfer rate increases with rise of magnetic parameter Ha and decreases with

rise in Casson parameter β , whereas the opposite trend is observed at the left wall of the channel.

The effect of Hall parameter β_h and Ion-slip parameter β_i on non-dimensional skin friction coefficient, heat and mass transfer rates against mixed convection parameter are plotted in Figs. 5(a)–5(c). Figure 5(a) exhibits that for both opposing and aiding flow cases, the skin friction coefficient decreases at the left wall and increases at the right wall with sequential increase in Hall and Ion-slip parameters. Figure 5(b) reveals that as Hall and Ion-slip parameters rises consecutively, the heat transfer rate shows opposite trend at both left and right walls in both opposing and aiding flow situations. Figure 5(c) portrays that for both opposing and aiding flow cases, the mass transfer rate enhances at the left wall and diminish at the right wall with increase of Hall and Ion-slip parameters.

The influence of Soret parameter S_r and Brinkman parameter Br on non-dimensional skin friction coefficient, heat and mass transfer rates against mixed convection parameter are displayed in Figs. 6(a)–6(c). From Fig. 6(a), we perceive that as Soret and Brinkman parameters increases, the skin friction coefficient show reverse trend in opposing and aiding flow situations at both walls of the channel. Figure 6(b) represents that with enhancement of Soret and Brinkman parameters, the heat transfer rate decreases at the left wall of the channel and increases at the right wall of the channel. For both aiding and opposing flow situations Fig. 6(c) illustrates that at both the walls of the channel, the mass transfer rate depicts reverse trend with an increment in Soret and Brinkman numbers.

Figs. 4(a)–6(c) prepared to analyze the effect of mixed convection parameter λ in Casson fluid. From these figures, it is found that the skin friction coefficient at the left wall of the channel is less in the opposing flow ($\lambda < 0$) in comparison with the aiding flow ($\lambda > 0$). The opposite nature is true at the right wall of the channel. The heat and mass transfer rates at the left wall of the channel is more in the opposing flow situation ($\lambda < 0$) and less in the aiding flow situation ($\lambda > 0$). The reverse behavior is found at the right wall of the channel.

6 Conclusions

This paper analyzes combined effects of viscous dissipation and Soret on the mixed convection flow of an electrically conducting Casson fluid by taking into account the Hall and Ion-slip effects. The resulting equations are solved analytically by Homotopy Analysis Method. The features of flow characteristics are analysed by plotting

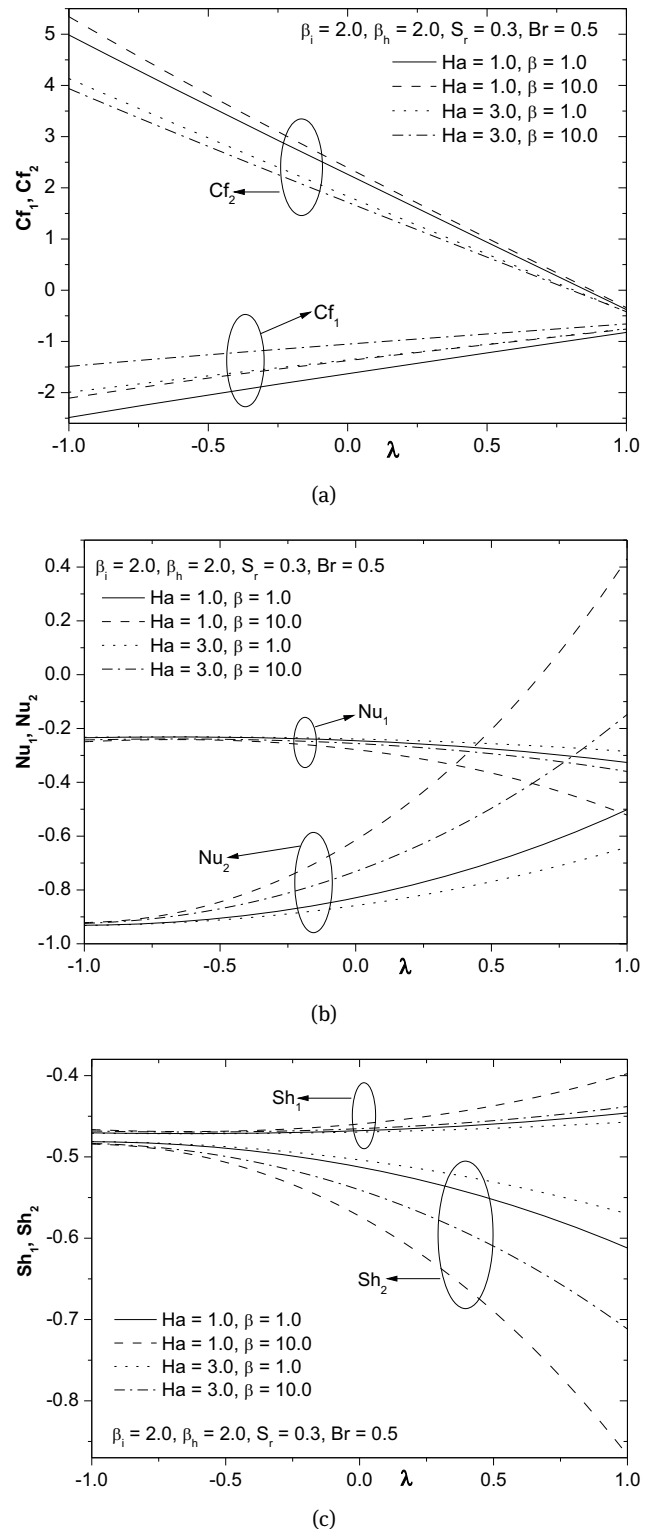


Fig. 4: Effect of Ha and β on (a) skin friction, (b) heat transfer rate, (c) mass transfer rate profiles at both the walls of the channel.

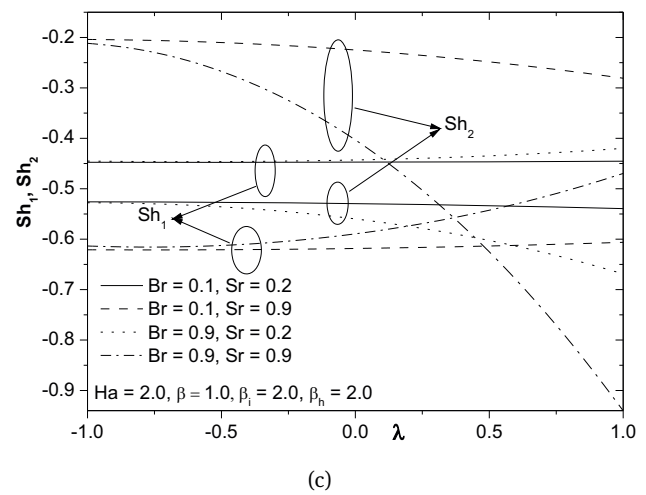
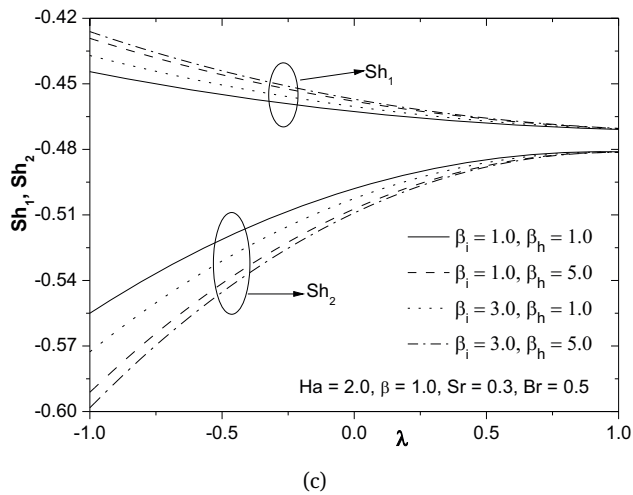
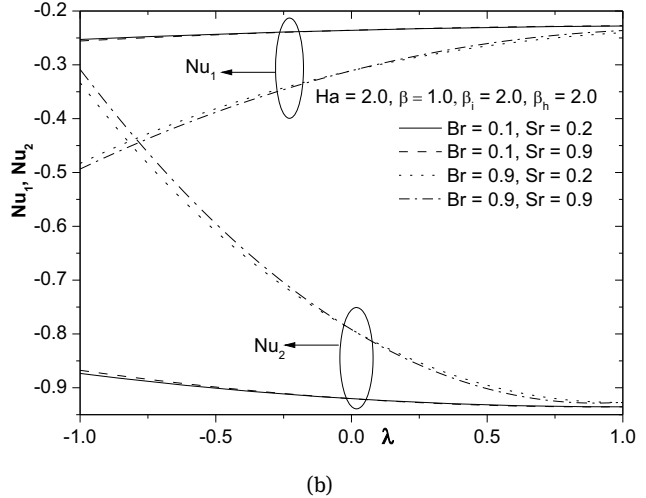
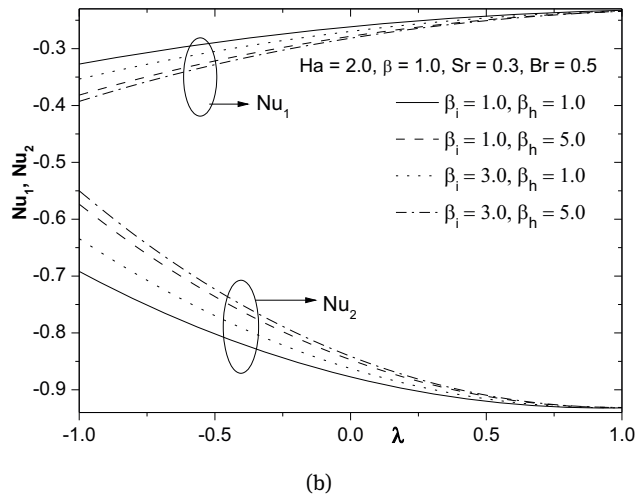
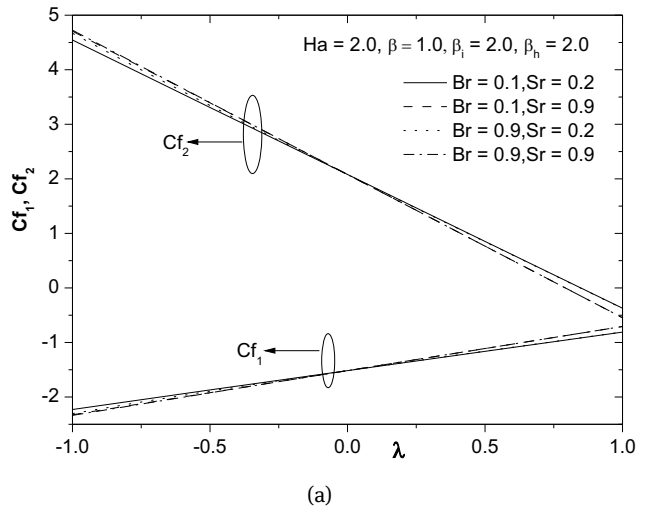
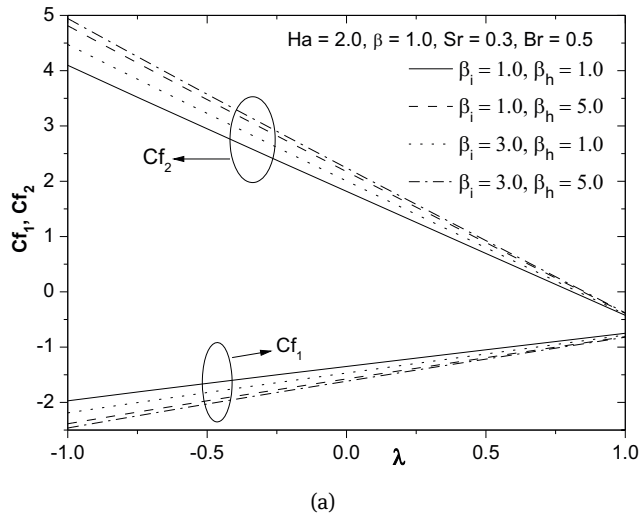


Fig. 5: Effect of β_i and β_h on (a) skin friction, (b) heat transfer rate, (c) mass transfer rate profiles at both the walls of the channel

Fig. 6: Effect of Br and Sr on (a) skin friction, (b) heat transfer rate, (c) mass transfer rate profiles both the walls of the channel.

graphs and discussed in detail. Influence of the viscous dissipation, Soret, Hall and Ion-slip effects on mixed convection in a Casson fluid, enhanced the number of non-dimensional parameters considerably thereby increasing the complexity of the present problem. The main findings are summarized as follows:

- Increasing the values of Casson fluid parameter, enhanced the surface shear stress at both the walls of the channel, diminished the heat transfer rate at left wall but enhanced at right wall of the channel whereas, the opposite trend is found in the case of mass transfer rate.
- In aiding and opposing flow situations, with an increase of magnetic parameter the skin friction coefficient and heat transfer rate are enhanced but mass transfer rate is diminished at the left wall whereas, it shown reverse trend at the right wall.
- As Hall and Ion slip parameter rise, it is found that the mass transfer rate is enhanced, skin friction coefficient and heat transfer rate are decreased at the left wall and depicted the opposite trend at the right wall for both aiding and opposing flows.
- The non-dimensional skin friction and heat transfer rate shown opposite trend in both opposing and aiding flows with the increase of Soret and Brinkman numbers. Further, the mass transfer rate displayed reverse trend at left and right walls for opposing and aiding flows.

References

- [1] Tao LN. On combined free and forced convection in channels. *Journal of Heat Transfer* 1960, 233–238.
- [2] Barletta A. Laminar mixed convection with viscous dissipation in a vertical channel. *International Journal of Heat and Mass Transfer* 1998, 41(22), 3501–3513.
- [3] Cheng CH, Kou HS, Huang WH. Flow reversal and heat transfer of fully developed mixed convection in vertical channels. *Journal of Thermophysics* 1990, 4(3), 375–383.
- [4] Kumar L, Bhargava R, Bhargava P, Takhar HS. Finite element solution of mixed convection micropolar fluid flow between two vertical plates with varying temperature. *Archives of Mechanics* 2005, 57, 251–264.
- [5] Srinivasacharya D, Shiferaw M. Numerical Solution to the MHD Flow of Micropolar Fluid Between Parallel Porous Plates. *International Journal of Fluid Mechanics Research* 2008, 35, 365–373.
- [6] Abdulaziz O, Noor NFM, Hashim I. Homotopy analysis method for fully developed MHD micropolar fluid flow between vertical porous plates. *International Journal for Numerical Methods in Engineering* 2009, 78, 817–827.
- [7] Sun H, Li R, Chenier E, Lauriat G. On the modeling of aiding mixed convection in vertical channels. *Heat Mass Transfer* 2012, 48, 1125–1134.
- [8] Singh KD. Effect of slip condition on viscoelastic MHD oscillatory forced convection flow in a vertical channel with heat radiation. *International Journal of Applied Mechanics and Engineering* 2013, 18(4), 1237–1248.
- [9] Alizadeh R, Bahambari AD, Rahmdel K. Mixed convection of Newtonian fluid between vertical parallel plates channel with MHD effect and variation in Brinkman number. *Acta Tehnica Corviniensis Bulletin of Engineering* 2014, 104–108.
- [10] Casson N. A flow equation for pigment-oil suspensions of the printing ink type. In: C.C.Mills (ed.), *Rheology of disperse systems*, Newyork, Oxford: Pergamon 1959, 84.
- [11] Tamamashi B. Consideration of certain hemorheological phenomena from the stand-point of surface chemistry in *Hemorheology* (A.L. Copley, ed.). Pergamon Press, London 1968, 89.
- [12] Walawander WP, Chen TY, Cala DF. An aproximate Casson fluid model for tube flow of blood. *Biorheology* 1975, 12, 111.
- [13] Batra RL, Jena B. Flow of a Casson fluid in a slightly curved tube. *International journal of engineering science* 1991, 29, 1245.
- [14] Das B, Batra RL. Secondary flow of a Casson fluid in a slightly curved tube. *International journal of non-linear mechanics* 1993, 28(5), 567.
- [15] Sayed Ahmed ME, Attia HA. Magnetohydrodynamic flow and heat transfer of a non-Newtonian fluid in an eccentric annulus. *Canadian Journal of Physics* 1998, 76, 391.
- [16] Nadeem S, Rizwan Ul Haq, Noreen Sher Akbar, Khan ZH. MHD three-dimensional Casson fluid flow past a porous linearly stretching sheet. *Alexandria Engineering Journal* 2013, 52(4), 577–582.
- [17] Mahanta G, Shaw S. 3D Casson fluid flow past a porous linearly stretching sheet with convective boundary condition. *Alexandria Engineering Journal* 2015, 54(3), 653–659.
- [18] McDonald DA. *Blood flows in arteries*, 2nd Edition, Chap. 2, London: Arnold 1974.
- [19] Shaw S, Gorla RSR, Murthy PVS, Ng CO. Pulsatile Casson fluid flow through a stenosed bifurcated artery. *International Journal of Fluid Mechanics Research* 2009, 36(1), 43–63.
- [20] Mukhopadhyay S. Casson fluid flow and heat transfer over a nonlinearly stretching surface. *Chinese Physics B* 2013, 22(7), 074701.
- [21] Kameswaran PK, Shaw S, Sibanda P. Dual solutions of Casson fluid flow over a stretching or shrinking sheet. *Sadhana* 2014, 39(6), 1573–1583.
- [22] Eckert ERG, Drake RM. *Analysis of heat and mass transfer*. McGraw-Hill, New York.
- [23] Dursunkaya Z, Worek WM. Diffusion-Thermo and Thermal-Diffusion Effects in Transient and Steady Natural Convection from Vertical Surface. *International Journal of Heat and Mass Transfer* 1992, 35(8), 2060–2065.
- [24] Srinivasacharya D, Kaladhar K. Soret and dufour effects on free convection flow of a couple stress fluid in a vertical channel with chemical reaction. *Chemical Industry and Chemical Engineering Quarterly* 2013, 19(1), 45–55.
- [25] RamReddy Ch, Murthy PVS, Chamkha AJ, Rashad AM. Soret effect on mixed convection flow in a nanofluid under convective boundary condition. *International Journal of Heat and*

- Mass Transfer 2013, 64, 384–392.
- [26] Srinivasacharya D, Mallikarjuna B, Bhuvanavijaya R. Soret and Dufour effects on mixed convection along a vertical wavy surface in a porous medium with variable properties. *Ain Shams Engineering Journal* 2015, 6(2), 553–564.
 - [27] Tani I. Steady flow of conducting fluids in channels under transverse magnetic fields with consideration of Hall effects. *Journal of Aerospace Science* 1962, 29, 297–305.
 - [28] Soundalgekar VM, Vighnesam NV, Takhar HS. Hall and ion-slip effects in MHD Couette flow with heat transfer. *Plasma Science, IEEE Transactions* 1979, 7(3), 178–182.
 - [29] Srinivasacharya D, Mekonnen Shiferaw. Hall and ion-slip effects on the flow of micropolar fluid between parallel plates. *International Journal of Applied Mechanics and Engineering* 2008, 13(1), 251–262.
 - [30] Srinivasacharya D, Mekonnen Shiferaw. MHD Flow of a Micropolar fluid in a rectangular duct with Hall and Ion slip effects. *Journal of the Brazilian Society of Mechanical Sciences and Engineering* 2008, 30(4), 313–318.
 - [31] Srinivasacharya D, Mekonnen Shiferaw. MHD flow of a micropolar fluid in a circular pipe with hall effects. *The ANZIAM Journal* 2009, 51, 277–285.
 - [32] Srinivasacharya D, Kaladhar K. Analytical solution for Hall and Ion-slip effects on mixed convection flow of couple stress fluid between parallel disks. *Mathematical and Computer Modelling* 2013, 57, 2494–2509.
 - [33] Garg BP, Singh KD, Bansal AK. Hall current effect on viscoelastic (Walter's liquid model-B) MHD oscillatory convective channel flow through a porous medium with heat radiation. *Kragujevac Journal of Science* 2014, 36, 19–32.
 - [34] Shakeri Askia F, Seyed Jalal Nasir Khanic, Mohammadiand E, Asgarie A. Application of Adomian decomposition method for micropolar flow in a porous channel. *Propulsion and Power Research* 2014, 3(1), 15–21.
 - [35] Liao SJ. *Beyond perturbation: Introduction to homotopy analysis method*. Chapman and Hall/CRC Press, and Boca Raton 2003.
 - [36] Liao SJ. On the homotopy analysis method for nonlinear problems. *Applied Mathematics and Computation* 2004, 147(2), 499–513.
 - [37] Liao SJ. An optimal homotopy-analysis approach for strongly nonlinear differential equations. *Communications in Nonlinear Science and Numerical Simulation* 2010, 15, 2003–2016.
 - [38] Liao SJ. On the relationship between the homotopy analysis method and Euler transform. *Communications in Nonlinear Science and Numerical Simulation* 2010, 14, 1421–1431.
 - [39] Turkyilmazoglu M. Numerical and analytical solutions for the flow and heat transfer near the equator of an MHD boundary layer over a porous rotating sphere. *International Journal of Thermal Sciences* 2011, 50, 831–842.